Applied Mathematics & Information Sciences
An International Journal

Analytical Solution to the Roof Bending Deflection with Mixed Boundary Conditions under Uniform Load

Shuren Wang[1,2] *and Zhongqiu Wang*[1]

[1] School of Civil Engineering and Mechanics, Yanshan University, Qinhuangdao, 066004, China
[2] Key Laboratory of Mechanical Reliability for Heavy Equipments and Large Structures, Qinhuangdao, 066004, China

Received: 8 Aug, 2012; Revised 10 Oct, 2012; Accepted 20 Oct, 2012
Published online: 1 Mar. 2013

Abstract: Analytical solution to the roof bending deflection is the key to conduct the stability evaluation and risk prediction of the shallow mined-out areas. The engineering mechanics model of the roof was built through the generalization engineering model of the practical shallow mined-out areas. Based on Reissner's thick plate theory, the roof bending deflection with mixed boundary conditions under uniform load was analyzed through the reciprocal theorem method. The function of roof bending deflection was derived and the analytical solution was verified by the numerical solution. Then, a comparative analysis was conducted for the difference characteristics of roof bending deflection with mixed boundary conditions and simply-supported boundary conditions.

Keywords: Mined-out areas, roof, mixed boundary conditions, Reissner's thick plate theory

1 Introduction

The deformation properties and instability mechanism of the roof in the shallow mined-out areas are the current challenging problems which should be worked out urgently in engineering practice [1].

Some scholars treat the roof as elastic rock beam for analytical analysis and research of the roof deformation characteristics of the mined-out areas. For example, X.Y. Zhang et al. [2] simplified the roof as elastic beam and analyzed the creep process on the base of the creeping damage theory. X.L. Jiang et al. [3] improved the beam model and discussed the influence to the roof thickness caused by horizontal stress and rock fractures based on structure stability theory and damage theory. S.Q. Qin et al. [4] regarded the roof as elastic beam and analyzed the instability process of mechanical system of stiff roof and coal pillar with catastrophe theory. G.M. Swift et al. [5] considered the roof as elastic beam and analyzed the stability factors to the roof in the mined-out areas. The differences between the elastic beam hypothesis and the practical roof made it difficult to reflect the actual conditions of the roof stress and its deformation.

Other scholars treated the roof as elastic thin plate in order to do such analysis and research. For example, R.H. Lin et al. [6] analyzed the overlying strata and obtained the strength condition of the key layer breaking instantly through the elastic thin slab theory and plastic limit analysis method. J.A. Wang et al. [7] regarded the roof as thin plate, analyzed the roof fracture process and its effect to the collapse of the mined-out areas. H. Li et al. [8] simplified the overlying strata of the steeply-inclined seam as thin plate, obtained the prediction deformation formula based on the thin plate bending theory with elasticity mechanics. X.Y. Lin et al. [9] treated the stiff roof as elastic thin plate to study the stress distribution rules and the fracture mechanism of the roof while considering the initial boundary conditions and the periodical ground pressure. H. Liu et al. [10] assumed the roof as thin plate and explored the stability of the stiff roof and pillar system. In practical engineering, it was limited to do the research using thin plate theory because the roof of the mined-out areas was usually in the state of the thick plate.

Although some scholars regarded the roof as thick plate and achieved some conclusions [11-13], the numerous problems need to be solved urgently with the development of the engineering practice. Therefore, the authors assumed the roof as thick plate and analyzed the characteristic of roof bending deflection with mixed boundary condition

* Corresponding author: e-mail: w_sr88@163.com

under uniform load by the reciprocal theorem method based on Reissner's thick plate theory in order to provide the technological supports for practical projects.

2 Building computational model

In the northeast edge of Antaibao Surface Mine, there was the mined-out areas of Jingyang Mine exploited by the room-and-pillar stoping method. Based on the field investigation and the collected information, the engineering model of the mined-out areas was built as in Fig.1.

The hypothesis of the roof was usually regarded as the thick plate with simply supported or with four edges fixed, which were different with the real boundary conditions. Thus, it was more appropriate to simplify the roof as the thick plate with mixed boundary conditions (Fig.1b) and the engineering mechanics model was showed in Fig.2.

The engineering mechanics model was assumed that the long side of the thick rectangular plate is *a*, the short side is *bba)*, the supporting length along the long side direction of the plate is a_1 ,the free length is *s*, the supporting length along the short side direction is b_1 , the free length is *l*. The thickness of the roof is *h*, its elastic modulus is *E*, and the poisson's ratio is *v*. The dead load of the overlying strata is regarded as uniform load *q* which is distributed on the upper surface of the roof. Thus, the engineering mechanics model was generalized as in Fig.2.

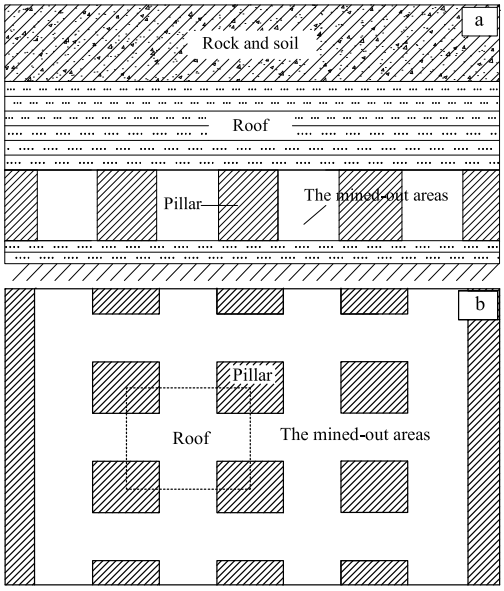

Fig. 1 The sketch of engineering model.(a)Section map of the mined-out areas;(b)Overhead view of the mined-out areas

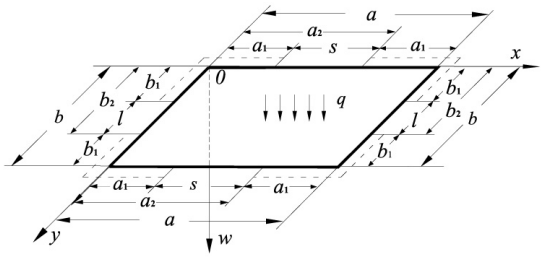

Fig. 2 The sketch of engineering mechanics model (Real system of thick plate with mixed boundary).

3 Deriving formulas as for the roof bending deflection with mixed boundary conditions

3.1 Basic equation

On the base of Reissner's thick plate theory, the basic static equations are showed as follows:

$$D\nabla^4 W = q(x,y) - \frac{2-\nu}{1-\nu}\frac{h^2}{10}\nabla^2 q(x,y) \tag{1}$$

$$\nabla^2\varphi - \left({}^{10}/_{h^2}\right)\varphi = 0 \tag{2}$$

where *D* is the flexural rigidity of the roof, is Laplace operator, *W* is the deflection of the roof, *q*(x,y) is the uniform load distributed on the roof, *v* is the Poisson's ratio, *h* is the thickness of the roof, and φ is the stress function.

$$D = Eh^3/\left[12\left(1-\upsilon^2\right)\right] \tag{3}$$

where *E* is the elastic modulus of the roof.

3.2 Basic system of the thick plate

Fig.3 shows the basic system of the thick rectangular plate with simply supported under concentrated loads, that is, the transverse two-dimensional Dirack-Delta function $(x-\xi, y-\eta)$ acts in the convective coordinate (ξ,η) of the thick plate with four edges simply supported. And $w_{1,x0}$, $w_{1,xa}$, $w_{1,y0}$, and $w_{1,yb}$ are the four-sided rotation angles of the basic system respectively. V_{1x0}, V_{1xa}, V_{1y0}, and V_{1yb} are the equivalent shear forces respectively. R_{100}, R_{1a0}, R_{1ab}, and R_{10b} are the corner loads respectively .

3.3 Real system of the thick plate

Fig.2 shows the thick plate with the central free and the rest simply supported of four edges under uniform load, that is, the real system of thick rectangular plate with mixed boundary. And deflections and twist angles are w_{x0}, w_{xa}, w_{y0}, w_{yb}, ω_{x0}, ω_{xa}, ω_{y0}, and ω_{yb} respectively. For the real symmetric system, the deflection w_{y0} and twist angle ω_{y0}

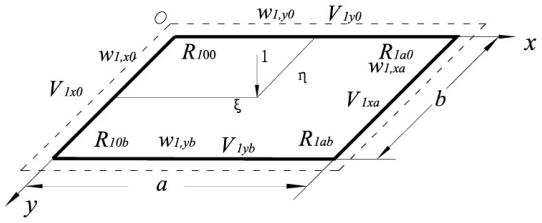

Fig. 3 Basic system for the thick rectangular plate.

on free boundary y=0 are equal to w_{yb} and ω_{yb} on free boundary y=b, and the deflection w_{x0} and twist angle ω_{x0} on free boundary x=0 are equal to w_{xa} and ω_{xa} at free boundary x=a. Thus, the deflection formula is written as follows:

$$W = W(\xi, \eta) \tag{4}$$

The deflection equations are

$$w_{y0} = w_{yb} = \sum_{i=1,3}^{\infty} A_i \cdot \sin \frac{i\pi(x - a_1)}{s} \tag{5}$$

$$w_{x0} = w_{xa} = \sum_{j=1,3}^{\infty} B_j \cdot \sin \frac{j\pi(y - b_1)}{l} \tag{6}$$

The twist angles are

$$\omega_{yx0} = \omega_{yxa} = \sum_{k=1,3}^{\infty} C_k \cdot \sin \frac{k\pi(y - b_1)}{l} \tag{7}$$

$$\omega_{xy0} = \omega_{xyb} = \sum_{f=1,3}^{\infty} D_f \cdot \sin \frac{f\pi(x - a_1)}{s} \tag{8}$$

where $x \in [a_1, a_2]$, $y \in [b_1, b_2]$, $a_2 = a_1 + s$, $b_2 = b_1 + l$. The stress function is

$$\begin{aligned} &\varphi(\xi, \eta) \\ &= \sum_{n=1,3}^{\infty} [E_n \cosh \delta_n \xi + F_n \cosh \delta_n (a - \xi)] \cos \beta_n \eta \\ &+ \sum_{m=1,3}^{\infty} [G_m \cosh \gamma_m \eta + H_m \cosh \gamma_m (b - \eta)] \cos \alpha_m \xi \end{aligned} \tag{9}$$

where $\alpha_m = \frac{m\pi}{a}$, $\beta_n = \frac{n\pi}{b}$, $\gamma_m = \sqrt{{\alpha_m}^2 + \frac{10}{h^2}}$, $\delta_n = \sqrt{\beta_n^2 + \frac{10}{h^2}}$ $A_i, B_j, C_k, D_f, E_n, F_n, G_m$, and H_m are undetermined coefficients respectively.

3.4 Driving the deflection equation

The reciprocal theorem method is used between the basic system and the real system, and the result is written as follows:

$$\begin{aligned} &W(\xi, \eta) + \int_{a_1}^{a_2} Q_{1yb} w_{yb} dx - \int_{a_1}^{a_2} Q_{1y0} w_{y0} dx \\ &+ \int_{b_1}^{b_2} Q_{1xa} w_{xa} dy - \int_{b_1}^{b_2} Q_{1x0} w_{x0} dy \\ &+ \int_{a_1}^{a_2} M_{1xyb} \omega_{xyb} dx - \int_{a_1}^{a_2} M_{1xy0} \omega_{xy0} dx \\ &+ \int_{b_1}^{b_2} M_{1yxa} \omega_{yxa} dy - \int_{b_1}^{b_2} M_{1yx0} \omega_{yx0} dy \\ &= \int_0^a \int_0^b q W_1(x, y; \xi, \eta) dx dy \end{aligned} \tag{10}$$

Substituting the related boundary values Eq. (5) to Eq. (8) of the real system, the related boundary values Q_{1y0}, $Q_{1yb}, Q_{1x0} Q_{1xb}, M_{1xy0}, M_{1xyb}, M_{1yx0}, M_{1yxa}$, and the basic solution $W_1(x, y, \xi, \eta)$ [14] of the basic system into Eq. (10). Then the deflection equation is reached as follows after calculating:

$$\begin{aligned} &W(\xi, \eta) = \frac{4q}{Da} \sum_{m=1,3}^{\infty} \{1 + \frac{1}{2 \cosh \frac{1}{2} \alpha_m b} [\alpha_m (\eta - \frac{b}{2}) \\ &\cdot \sinh \alpha_m (\eta - \frac{b}{2}) - (2 + \frac{1}{2} \alpha_m \tanh \frac{1}{2} \alpha_m b) \\ &\cdot \cosh \alpha_m (\eta - \frac{b}{2})]\} \frac{1}{\alpha_m^5} \sin \alpha_m \xi - \frac{2l}{\pi b} \sum_{j=1,3}^{\infty} j B_j \sum_{n=1,3}^{\infty} \\ &\frac{[\sinh \beta_n (a - \xi) + \sinh \beta_n \xi] \sin \beta_n \eta}{\sinh \beta_n a} \phi_{jn}(b, l) - \frac{2s}{\pi a} \\ &\cdot \sum_{i=1,3}^{\infty} i A_i \sum_{m=1,3}^{\infty} \frac{[\sinh \alpha_m (b - \eta) + \sinh \alpha_m \eta]}{\sinh \alpha_m b} \phi_{im}(a, s) \\ &+ \frac{(1 - \upsilon)}{\pi} \sum_{n=1,3}^{\infty} \{\beta_n a \coth \beta_n a [\sinh \beta_n (a - \xi) + \\ &\sinh \beta_n \xi] - \beta_n \xi \cosh \beta_n \xi - \beta_n (a - \xi) \cosh \beta_n (a - \xi)\} \\ &\cdot \frac{n \sin \alpha_m \xi}{\alpha_m \sinh \alpha_m b} \sum_{k=1,3}^{\infty} C_k H_{nk}(b, l) + \frac{(1 - \upsilon)}{\pi} \\ &\cdot \sum_{m=1,3}^{\infty} \{[\sinh \alpha_m (b - \eta) + \sinh \alpha_m \eta] \alpha_m b \cot \alpha_m b \\ &- \alpha_m (b - \eta) \cosh \alpha_m (b - \eta) - \alpha_m \eta \cosh \alpha_m \eta\} \\ &\cdot \frac{m \sin \beta_n \eta}{\beta_n \sinh \beta_n a} \sum_{f=1,3}^{\infty} D_f H_{mf}(a, s) \end{aligned} \tag{11}$$

where

$$\phi_{im}(a, s) = \frac{(-1)^i \sin \frac{a_1 + s}{a} m\pi - \sin \frac{a_1}{a} m\pi}{i^2 - (\frac{s}{a} m)^2} \tag{12}$$

$$\phi_{jn}(b, l) = \frac{(-1)^j \sin \frac{b_1 + l}{b} n\pi - \sin \frac{b_1}{b} n\pi}{j^2 - (\frac{l}{b} n)^2} \tag{13}$$

$$H_{mf}(a, s) = \frac{(-1)^f \sin \frac{a_1 + s}{a} m\pi - \sin \frac{a_1}{a} m\pi}{m^2 - (\frac{a}{s} f)^2} \tag{14}$$

$$H_{nk}(b, l) = \frac{(-1)^k \sin \frac{b_1 + s}{a} n\pi - \sin \frac{b_1}{a} n\pi}{n^2 - (\frac{b}{l} k)^2} \tag{15}$$

The boundary conditions of the real system are as follows : $\eta = 0, b$ and $\xi \in [a_1, a_2]$: $M_{\xi\eta}$=0, Q_η =0, M_η=0; ξ = 0,a and $\eta \in [b_1, b_2]$: $M_{\eta\xi}$=0,Q_ξ=0, M_ξ=0.

Due to the twist angles assumed in the corners of each edge, that is ω_{x0}, ω_{xa}, ω_{y0}, and ω_{yb}. The related equations on the boundary should be satisfied η = 0,b and $\xi \in [a_1, a_2]$: ω_ξ=$\omega_{\xi\eta 0}$; ξ=0,a and $\eta \in [b_1, b_2]$: ω_η=$\omega_{\eta\xi 0}$.

where M_η=0 , M_ξ=0 have been satisfied. For the symmetric conditions E_n=$-F_n$, G_m=$-H_m$. Therefore, we can get six equations according to the above mentioned six boundary conditions and obtain six undetermined coefficients. The deflection, shear, moment and rotation angel are showed as follows:

$$\frac{4q}{b}\frac{\tanh\frac{a\beta_n}{2}}{\beta_n^2}+\frac{16D(\nu-1)}{b\pi}\sum_{m=1,3}^{\infty}\frac{{\beta_n}^2 m\alpha_m^2}{\alpha_m^2+{\beta_n}^2}\sum_{f=1,3}^{\infty}D_f \cdot\frac{\sin\frac{m\pi a_1}{a}}{m^2-(\frac{af}{s})^2}+\frac{4D(\nu-1)}{\pi}\frac{(1-\cosh\beta_n a)n{\beta_n}^2}{\sinh\beta_n a} \cdot\sum_{k=1,3}^{\infty}C_k\frac{\sin\frac{n\pi b_1}{b}}{n^2-(\frac{bk}{l})^2}-E_n\beta_n(1-\cosh\delta_n a) +\frac{4}{b}\sum_{m=1,3}^{\infty}\frac{G_m\beta_n\gamma_m\sinh\gamma_m b}{\alpha_m{}^2+\beta_n{}^2}=0$$

$n = 1, 3...$ (16)

$$\frac{4q}{a}\frac{\tanh\frac{b\alpha_m}{2}}{\alpha_m{}^2}+\frac{16D(\nu-1)}{a\pi}\sum_{n=1,3}^{\infty}\frac{{\beta_n}^2 n\alpha_m{}^2}{\alpha_m{}^2+\beta_n{}^2}\sum_{k=1,3}^{\infty} C_k\frac{\sin\frac{n\pi b_1}{b}}{n^2-(\frac{bk}{l})^2}+\frac{4D(\nu-1)}{\pi}\frac{(1-\cosh\alpha_m b)m\alpha_m{}^2}{\sinh\alpha_m b} \cdot\sum_{f=1,3}^{\infty}D_f\frac{\sin\frac{m\pi a1}{a}}{m^2-(\frac{af}{s})^2}+G_m\alpha_m(1-\cosh\gamma_m b) -\frac{4}{a}\sum_{m=1,3}^{\infty}\frac{E_n\alpha_m\delta_n\sinh\delta_n a}{\alpha_m{}^2+\delta_n{}^2}=0$$

$m = 1, 3...$ (17)

$$\frac{16}{\pi^2}\sum_{m=1,3}^{\infty}m\alpha_m\sum_{i=1,3}^{\infty}iA_i\frac{(\sin\frac{m\pi a_1}{a})^2}{[i^2-(\frac{sm}{a})^2][m^2-(\frac{af}{s})^2]}+ \frac{16h^2a}{5s\pi^2}\sum_{m=1,3}^{\infty}m^2\alpha_m{}^2D_f\frac{(\sin\frac{m\pi a_1}{a})^2}{[m^2-(\frac{af}{s})^2]^2}- \frac{4ah^2}{5D\pi s(1-\upsilon)}\sum_{m=1,3}^{\infty}mG_m\gamma_m\sinh\gamma_m b\frac{\sin\frac{m\pi a_1}{a}}{m^2-(\frac{af}{s})^2} +D_f=0 \qquad f=1,3... \quad (18)$$

$$\frac{16}{\pi^2}\sum_{n=1,3}^{\infty}n\beta_n\sum_{j=1,3}^{\infty}jB_j\frac{(\sin\frac{n\pi b_1}{b})^2}{[j^2-(\frac{nl}{b})^2][n^2-(\frac{bk}{l})^2]}+ \frac{16h^2b}{5l\pi^2}\sum_{n=1,3}^{\infty}n^2\beta n^2C_k\frac{(\sin\frac{n\pi b_1}{b})^2}{[n^2-(\frac{bk}{l})^2]^2}-\frac{4bh^2}{5D\pi l(1-\upsilon)} \cdot\sum_{n=1,3}^{\infty}nE_n\delta n\sinh\delta_n a\frac{\sin\frac{n\pi b_1}{b}}{n^2-(\frac{bk}{l})^2}+C_k=0$$

$k = 1, 3...$ (19)

$$\frac{2q}{b}\{\frac{(1-\upsilon)}{\beta_n^3}(\tanh\frac{\beta_n a}{2}-\frac{\beta_n a}{2\cosh^2\frac{\beta_n a}{2}})- \frac{\upsilon h^2\tanh\frac{\beta_n a}{2}}{5\beta_n}\}=D(1-\upsilon)\frac{16s}{ab\pi}\sum_{m=1,3}^{\infty}\frac{\alpha_m{}^3}{\alpha_m{}^2+\beta_n{}^2} \cdot\sum_{i=1,3}^{\infty}iA_i\frac{\sin\frac{m\pi a_1}{a}}{i^2-(\frac{sm}{a})^2}+D(1-\upsilon)\frac{4l}{b\pi}\tanh\frac{\beta_n a}{2}{\beta_n}^2 \cdot\sum_{j=1,3}^{\infty}jB_j\frac{\sin\frac{n\pi b_1}{b}}{j^2-(\frac{nl}{b})^2}-D(\upsilon-1)^2\frac{16}{b\pi}\sum_{m=1,3}^{\infty} \frac{m\alpha_m{}^2\beta_n{}^2}{(\alpha_m{}^2+\beta_n{}^2)^2}\sum_{f=1,3}^{\infty}D_f\frac{\sin\frac{m\pi a_1}{a}}{m^2-(\frac{af}{s})^2}+D(1-\upsilon) \cdot\frac{16h^2}{5b\pi}\sum_{m=1,3}^{\infty}\frac{m\alpha_m{}^4}{\alpha_m{}^2+\beta_n{}^2}\sum_{f=1,3}^{\infty}D_f\frac{\sin\frac{m\pi a_1}{a}}{m^2-(\frac{af}{s})^2} +D(1-\upsilon)\frac{4h^2}{5\pi}n\beta_n{}^3\tanh\frac{\beta_n a}{2}\sum_{k=1,3}^{\infty}C_k\frac{\sin\frac{n\pi b_1}{b}}{n^2-(\frac{bk}{l})^2} -D(\upsilon-1)^2\frac{2n}{\pi}[\beta_n^2 a+\beta_n(1-\beta_n a\coth\beta_n a) \cdot\tanh\frac{\beta_n a}{2}]\sum_{k=1,3}^{\infty}C_k\frac{\sin\frac{n\pi b_1}{b}}{n^2-(\frac{bk}{l})^2}+\frac{h^2}{5}E_n({\beta_n}^2+{\delta_n}^2) \cdot\sinh^2\frac{\delta_n a}{2}-\frac{2h^2}{5b}\sum_{m=1,3}^{\infty}G_m\frac{\alpha_m{}^2+\gamma_m{}^2}{\gamma_m{}^2+\beta_n{}^2}\gamma_m\sinh\gamma_m b$$

$n = 1, 3\cdots$ (20)

$$\frac{2q}{a}\{\frac{(1-\upsilon)}{\alpha_m^3}(\tanh\frac{\alpha_m b}{2}-\frac{\alpha_m b}{2\cosh^2\frac{\alpha_m b}{2}})- \frac{\upsilon h^2\tanh\frac{\alpha_m b}{2}}{5\alpha_m}\}=D(1-\upsilon)\frac{4s}{a\pi}\tanh\frac{\alpha_m b}{2}\alpha_m{}^2\sum_{i=1,3}^{\infty}i \cdot A_i\frac{\sin\frac{m\pi a_1}{a}}{i^2-(\frac{sm}{a})^2}+D(1-\upsilon)\frac{16l}{ab\pi}\sum_{n=1,3}^{\infty}\frac{\beta_n{}^3}{\alpha_m{}^2+\beta_n{}^2} \cdot\sum_{j=1,3}^{\infty}jB_j\frac{\sin\frac{n\pi b_1}{b}}{j^2-(\frac{nl}{b})^2}-D(\upsilon-1)^2\frac{16}{a\pi}\sum_{n=1,3}^{\infty} \cdot\frac{n\alpha_m{}^2\beta_n{}^2}{(\alpha_m{}^2+\beta_n{}^2)^2}\sum_{k=1,3}^{\infty}C_k\frac{\sin\frac{n\pi b_1}{b}}{n^2-(\frac{bk}{l})^2}+D(1-\upsilon)\frac{16h^2}{5a\pi} \cdot\sum_{n=1,3}^{\infty}\frac{n\beta_n{}^4}{\alpha_m{}^2+\beta n^2}\sum_{k=1,3}^{\infty}C_k\frac{\sin\frac{n\pi b_1}{b}}{n^2-(\frac{bk}{l})^2}+D(1-\upsilon) \cdot\frac{4h^2}{5\pi}m\alpha_m{}^3\tanh\frac{\alpha_m b}{2}\sum_{f=1,3}^{\infty}D_f\frac{\sin\frac{m\pi a_1}{a}}{m^2-(\frac{af}{s})^2}-(\upsilon-1)^2$$

$$\cdot D\frac{2m}{\pi}[{\alpha_m}^2 b+\alpha_m(1-\alpha_m b\coth\alpha_m b\tanh\frac{\alpha_m b}{2}]$$
$$\cdot\sum_{f=1,3}^{\infty}D_f\frac{\sin\frac{m\pi a_1}{a}}{m^2-(\frac{af}{s})^2}-\frac{h^2}{5}G_m({\gamma_m}^2+{\alpha_m}^2)$$
$$\cdot\sinh^2\frac{\gamma_m b}{2}+\frac{2h^2}{5a}\sum_{n=1,3}^{\infty}E_n\frac{{\delta_n}^2+{\beta_n}^2}{{\alpha_m}^2+{\beta_n}^2}\beta_n\sinh\beta_n a$$
$$m=1,3\cdots \tag{21}$$

Solving the equations from Eq. (16) to Eq. (21) to get the coefficients A_i, B_j, C_k, D_f, E_n and G_m, and then the deflection, shear, moment and rotation angel can be worked out.

As a numerical example, the model was assumed that side length of a square thick plate is a=b=10 m, the length of simply supported edge is a_1=b_1=3 m, the length of free section is s=l=3 m. The poison's ratio of the plate is v=0.3, and its elastic modulus is E =50 GPa. The uniform load acing on the plate is q=0.3MPa . The deflection is supposed to obtain when the width-thickness ratio is h/a=0.1, 0.2 , 0.3.

According to the above equations, it is easy to get the deflection values of any place by using software MATLAB. Under the software MATLAB environment, the deflection values along the z direction can be reached when the points x/a=0.5, y/b=0.1, 0.2,$\cdots$ 1.0; x=0, y/l=0.1, 0.2,$\cdots$ 1.0 are chosen respectively.

In the solving process of coefficient equations set, the approximation solution with sufficient accuracy can be obtained through picking up the finite terms as shown in Table 1. So, the satisfactory results are obtained to keep relative errors less than 0.05 through calculation when c (c means the coefficients m, n, i, j, k, f) is equal to 80 respectively.

Table 1 The maximum deflection values and the relative errors of thick plate at x/a=0.5 and y/b=0.5 with different c.

	c =40		c =60		c =80	
ANSYS (mm)	W (mm)	*Error* (%)	W (mm)	*Error* (%)	W (mm)	*Error* (%)
3.45	3.58	3.97	3.54	2.77	3.52	2.12
0.51	0.54	6.69	0.53	5.48	0.53	4.54
0.20	0.21	5.22	0.21	4.06	0.21	3.55

4 Results and analysis

4.1 Verification for analytical solution

The thick plate with mixed boundary condition under uniform load is simulated by using ANSYS. A square plate with side length a=b=10 m is selected, and the thickness-width ratio is h/a=0.1, 0.2, and 0.3 respectively. The numerical model was computed under the same condition under the uniform loads being applied, and the displacement of z direction can be obtained, that is, the deflection values of the roof of the mined-out areas.

As showed in Fig.4 and Fig.5, the deflection curves of the thick plate at x/a=0.5 and at x=0 with different thickness-width ratios had been worked out respectively.

The result indicates that whether on the boundary or in the place of the deflection maximum, the error is less than 0.05 between the numerical solution and the analytical solution, which is acceptable in the practical engineering.

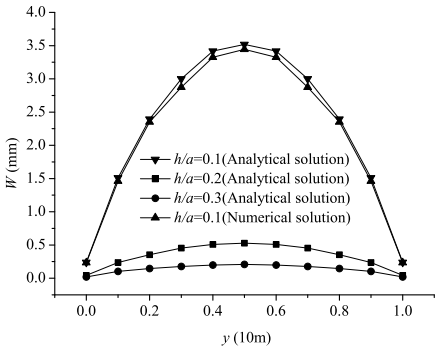

Fig. 4 The deflection curves of thick plate at x/a=0.5.

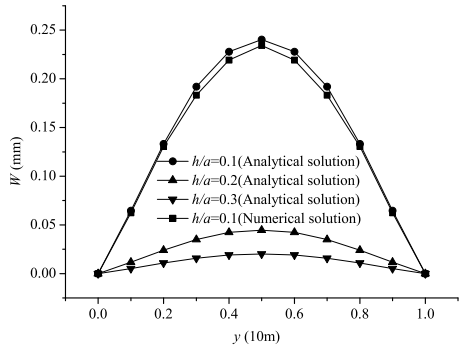

Fig. 5 The deflection curves of the free section of thick plate at x/a=0.

4.2 Comparative analysis of two different boundary conditions

The square plates of side length a=b=10 m with simply-supported of four edges and with mixed boundary conditions are selected, and the length of free sections and the simply-supported sections of the thick plate with mixed boundary conditions are a_1=b_1=3 m, and s=l=3 m respectively. Uniform load q being applied on the upper surface

of the plate is equal to 0.3 MPa. The poison's ratio of the plate is v=0.3, and its elastic modulus is E=50 GPa, The thickness-width ratio of the plate is h/a=0.1, 0.2, and 0.3 respectively. The results are showed in Fig.6 ,Fig.7 and Fig.8.

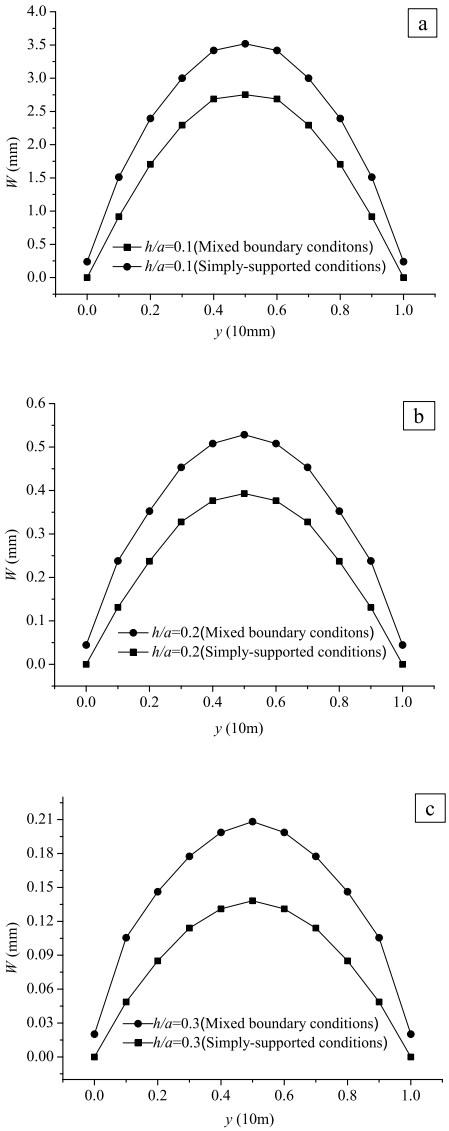

Fig. 6 The deflection curves of thick plate at x/a=0.5. (a) h/a=0.1; (b) h/a=0.2; (c) h/a=0.3

5 Conclusion

Based on Reissner's thick plate theory, the roof bending deflection with mixed boundary conditions in the mined-out areas under uniform load was analyzed through the reciprocal theorem method. The function of roof bending deflection was derived and the analytical solution was worked out.

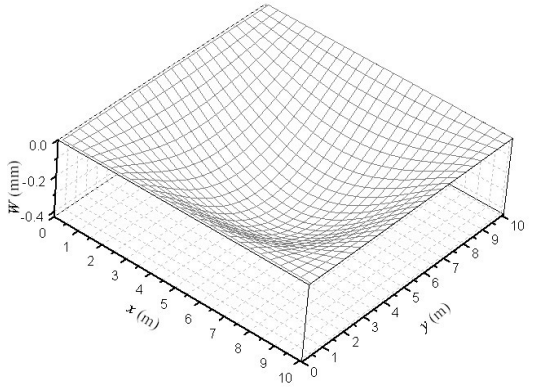

Fig. 7 The deflection surface of h/a=0.2 thick plate with simply-supported boundary conditions.

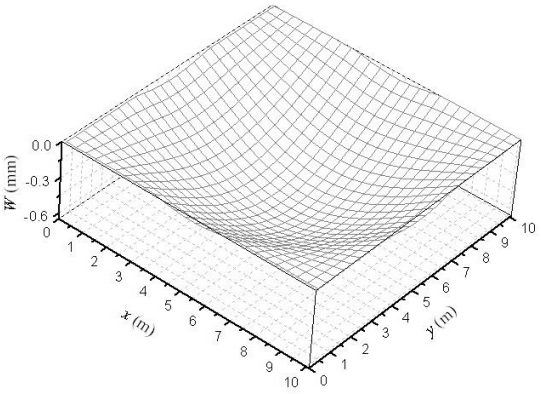

Fig. 8 The deflection surface of h/a=0.2 thick plate with mixed boundary conditions.

Comparing the numerical solution with the analytical solution, the thick plate theory is appropriate for analyzing the characteristic of roof bending deflection under the same condition.

Through analyzing the difference characteristics of roof bending deflection with two different boundary conditions, it is showed that roof bending deflection with mixed boundary conditions is bigger than that with simply-supported boundary conditions, and the deformation scope of roof bending deflection with mixed boundary conditions is apparently greater than that of simply-supported boundary conditions with increase of the thickness-width ratio.

Acknowledgement

This work was financially supported by the National Natural Science Foundation of China (No:51074140).

References

[1] Wang, S.R., Jia, H.H. and C.F. Wu, Determination method of roof safety thickness in the mined out regions under dynamic loading and its application, Journal of China Coal Society, **35**, No. 8, 1263-1268 (2010).

[2] Zhang, X.Y. Analysis of creep damage fracture of upper roof, Journal of Liaoning Technical University (Natural Science), **28**, No. 5, 777-780 (2009).

[3] Jiang, X.L., Cao, P., Yang, H. and H. Lin, Effect of horizontal stress and rock crack density on roof safety thickness of underground area, Journal of Central South University (Science and Technology), **40**, No. 1, 211- 216 (2009).

[4] Qin, S.Q. and S.J. Wang, Instability leading to rockbursts and nonlinear evolutionary mechanisms for coal-pillar-and-roof system, Journal of Engineering Geology, **13**, No.4, 437-446 (2005).

[5] Swift, G.M. and D.J. Reddish, Stability problems associated with an abandoned ironstone mine, Bulletin of Engineering Geology and the Environment, **61**, No. 3, 227-239 (2002).

[6] Lin, H.F., Li, S.G., Cheng L.H. Key layer distinguishing method of overlying strata based on the thin slab theory , Journal of China Coal Society, **33**, No. 10, 1081-1085 (2008).

[7] Wang, J.A., Shang X.C. and H.T. Ma, Investigation of catastrophic ground collapse in Xingtai gypsum mines in China, International Journal of Rock Mechanics & Mining Sciences, **45**, No.8,1480-1499 (2008).

[8] Li, H., Liang, B., Li, G., Bai Y.P. and C.M. Zhang, Prediction on bending deflection of overlying strata caused by steeply-inclined coal seam mining in mountainous area, The Chinese Journal of Geological Hazard and Control, **21**, No. 3, 101-104 (2010).

[9] Li, X.Y., Gao F. and W.P. Zhong, Analysis of fracturing mechanism of stope roof based on plate model, Journal of Mining & Safety Engineering, No. 2, 180-183 (2008).

[10] Liu, H., Hu, Q.T., Wang J.A. and J.G. Li, Analysis on stability of pillar and stiff roof system in the gob area, Journal of Coal Science & Engineering, **15**, No. 2, 206-209 (2009).

[11] Zhu, F.C., Cao P. and W. Wan, Determination of safe roof thickness of underground shallow openings based on axisymmetric thick plate mode, Ground Pressure and Strata Control, **23**, No. 1, 115-118 (2006).

[12] He, G.L. Determination of critical thickness of stiff roof in coal mine based on thick plate theory, Chinese Journal of Underground Space and Engineering, **5**, No. 4, 659-663 (2009).

[13] Tan, W.F., Liu J.J. and B.L. Fu, Reciprocal theorem method for bending of thick rectangular plates supported at four corner points, Journal of Engineering Mechanics, **13**, No. 4, 49-58 (1996).

[14] B.L. Fu and W.F. Tan, Reciprocal theorem method for solving the problem of thick rectangular plates, Journal of Applied Mathematics and Mechanics, **16**, No. 4, 367-379 (1995).

Shuren Wang is one professor from the School of Civil Engineering and Mechanics, Yanshan University, China. He obtained his Ph.D. degree from University of Science and Technology (Beijing). And he has been worked as a visiting scholar at the School of Mining Engineering, the University of New South Wales, Australia. He is an active researcher in mining engineering, geotechnical engineering, soil mechanics and numerical simulation, and has published more than 50 research articles in journals of the related fields.

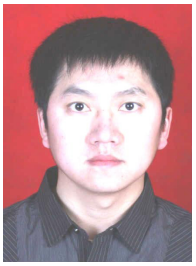

Zhongqiu Wang received the B.S. degree from the Shool of Engineering Technology, China University of Geosciences (Beijing), China. Now he is a master student at School of Civil Engineering and Mechanics, Yanshan University,China. His interested research is mining engineering and risk prediction of the shallow mine-out areas.